

The extraction behavior of organotin compounds is strongly influenced by solvent properties. Although solubility data show that DMT and MMT dissolve more effectively in methanol than in water, and tin oxides remain largely insoluble [2]-[5], these assumptions have not been validated for complex industrial residues. Moreover, the combined effects of solvent system, extraction duration, and agitation intensity have rarely been examined, leaving fundamental questions about tin dissolution kinetics unanswered.

A crucial knowledge gap lies in the absence of reliable kinetic modeling. While pseudo-first-order and pseudo-second-order models are widely applied in hydrometallurgical systems, their applicability to organotin dissolution has not been evaluated [6]. Past studies often relied on linearized kinetic plots, which may introduce bias due to data transformation. In contrast, non-linear regression allows the full kinetic profile to be fitted without distortion, producing more accurate estimates of rate constants (k) and equilibrium concentrations (C_s) [7].

In many solid-liquid extraction systems, the kinetic curve exhibits two characteristic regimes: a short-time regime, dominated by external mass transfer and strongly influenced by agitation and solvent accessibility; and a long-time regime, where the rate gradually slows due to intraparticle diffusion or diminishing concentration gradients [8]. Recognizing these regimes is essential for distinguishing whether tin dissolution is controlled by surface reaction or diffusion limitations, and for selecting the most appropriate kinetic model and regression method.

Given these gaps, this study aims to: (i) evaluate the extraction performance of DMT by-product using water, methanol, and methanol-water mixtures under varying agitation rates; (ii) determine kinetic parameters using both linearized and non-linear regression of pseudo-first order and pseudo-second-order models; and (iii) establish a validated kinetic model describing tin dissolution behavior. The outcomes are expected to provide a robust solvent-parameter matrix for optimizing tin recovery and support sustainable hydrometallurgical strategies aligned with Indonesia's tin downstream agenda and global circular-economy initiatives.

The expected outcomes of this research include: (i) a validated kinetic model representing the extraction behavior of organotin species from industrial by-products, (ii) a solvent process parameter matrix for optimizing tin recovery

2. MATERIALS AND METHODS

2.1 Materials

The main material used in this study was the DMT by-product collected from a single production line of the DMT unit at PT Timah Industri (Fig. 1). Analytical-grade methanol (>99.8% PA), 50% methanol solution, and deionized water were used as solvents for the solid-liquid extraction process. All chemicals in this study were used without further purification.



Figure 1. DMT by-product sample

2.2 Solid-liquid extraction of tin

The sample was prepared through grinding, sieving, and mixing to obtain a uniform particle maximum size of 10 mesh. A total of 50 g of sample was mixed with 500 mL of solvent under stirring at either 300 or 400 rpm. Three types of solvents were tested: deionized water, a 50:50 methanol-water mixture, and pure methanol. The extraction process was carried out for 24 hours at ambient temperature. Samples were collected at specific time intervals: 0, 2, 4, 8, 15, 30, 60, 120, 240, 480, 960, and 1440 minutes. The tin concentration in the liquid samples was determined using XRF (x-ray fluorescence) analysis with a Malvern Panalytical Epsilon 1 instrument operating in the 7-50 keV energy range.

For the analysis, liquid filtrates were poured into dedicated XRF (x-ray fluorescence) liquid cups sealed with a 3 μ m polypropylene thin film. This non-destructive method was selected due to the high concentration of tin in the samples (approximately 20–35%), which allowed for direct measurement without the extensive dilution required by ICP-OES (inductively coupled plasma-optical emission spectrometry) or AAS (atomic absorption spectrometry), thereby

minimizing potential dilution errors. Each experimental condition was performed in triplicate, and the reported data represents the average values of three independent runs.

2.3 Kinetic Modeling

In the extraction of tin from DMT by-product, the kinetics models tested for the research sample data were first-order and second-order kinetics. The first-order kinetics model is an equation that describes the value of the extraction rate, which is proportional to a driving force in the form of concentration ($C_s - C_t$), and this equation has a correlation to the linear driving force. In general, the equation is written in Eq. (1), while the second-order kinetics model assumes extraction influenced by surface adsorption-desorption and intraparticle diffusion in Eq. (2).

$$\frac{dC_t}{dt} = k(C_s - C_t) \quad \text{Eq. (1)}$$

$$\frac{dC_t}{dt} = k(C_s - C_t)^2 \quad \text{Eq. (2)}$$

For C_s is the concentration of tin when it reaches equilibrium (%), C_t is the concentration of tin at a certain time or extraction operation time (%), and k is the value of the extraction rate constant (min^{-1}). It can be made linearly in the form of Eq. (3) and Eq. (4) by integrating Eq. (1) and Eq. (2), with boundary conditions when $t = 0$; $C_t = 0$ and when $t = t$; $C_t = C_s$.

$$\ln(C_s - C_t) = \ln(C_s) - kt \quad \text{Eq. (3)}$$

$$\frac{t}{C_t} = \frac{1}{kC_s^2} + \frac{1}{C_s} t \quad \text{Eq. (4)}$$

For the first-order, the value of k can then be found by plotting t as the x-axis and $\ln(C_s - C_t)$ on the y-axis, while for the second-order, by plotting t/C_t vs t . It will provide a slope and intercept that can be used to find the value of the extraction rate constant of the first order (k).

While for the regression non-linear form, Eq. (5) and Eq. (6) are used for model fitting performed using software Microsoft Excel to obtain rate constant k and equilibrium concentration C_s [9], [10].

$$C_t = C_s (1 - e^{-kt}) \quad \text{Eq. (5)}$$

$$C_t = \frac{kC_s^2 t}{1 + kC_s t} \quad \text{Eq. (6)}$$

3. RESULTS AND DISCUSSION

3.1 Solid-liquid extraction of tin

The solid-liquid extraction process of the DMT by-product over 24 h with sampling at selected time intervals is presented in Fig. 2.

The concentration of tin increased progressively with longer extraction time. According to the last research [8], this trend arises

from the prolonged contact time between the solvent and solid, which enhances mass transfer. A rapid increase in tin concentration was observed during the initial stage, followed by a gradual rise and eventual plateau as the extraction progressed. The rapid-extraction stage occurs at the beginning of the process, where tin species are readily released. As time progresses, the extraction rate decreases and approaches a nearly constant tin concentration. This behavior is crucial for subsequent kinetic modeling. Figure 2 also shows clear variations in extraction performance depending on the solvent used. Each solvent exhibits significantly different extraction behavior.

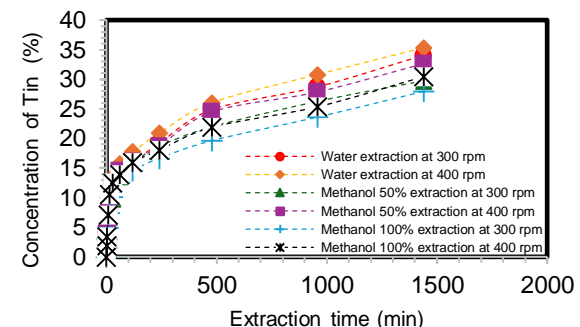


Figure 2. Extraction of tin (Sn) in DMTC-BP over time

Table 1 summarizes the average tin concentration obtained after 24 h. Water produced the highest tin concentration compared to 50% methanol and pure methanol. Increasing agitation speed from 300 to 400 rpm also enhanced extraction efficiency for all solvents, indicating the contribution of both solvent properties and hydrodynamic conditions. The average tin concentrations from triplicate experiments show that 400 rpm consistently produced higher tin concentrations than 300 rpm for all solvents. The highest tin concentration ($35.35 \pm 0.09\%$) was obtained using water, while the lowest ($27.96 \pm 0.71\%$) was obtained using pure methanol.

The two-way ANOVA results presented in Table 2 indicate that solvent type, agitation speed, and their interaction significantly affect the extraction performance. The F-value for solvent type (1184.69) is higher than the F-critical value of 2.48, with a P-value of 0.00 (<0.05), indicating a significant influence of solvent variation.

Table 1. Tin extraction yield: average result after 24 hours

Solvent Type	Stirring Speed	Final Tin Yield (%)
Water	300 rpm	34.07 ± 0.39
Water	400 rpm	35.35 ± 0.09
Methanol 50%	300 rpm	29.75 ± 3.62
Methanol 50%	400 rpm	32.65 ± 0.37

Methanol	300 rpm	27.96 ± 0.71
Methanol	400 rpm	30.45 ± 0.12

This suggests that the ability of solvents to dissolve or extract tin species from the DMT by-product differs according to their chemical characteristics.

Table 2. Analysis of variance of the experimental data for Tin (Sn) extraction

Source of Variation	F	P-value	F crit
Solvent types (a)	1184.69	0.00	2.48
Stirring speed (b)	252639.99	0.00	3.26
(a)*(b)	1109.18	0.00	2.11

Agitation speed shows the highest F-value ($252639.99 > 3.26$) with a P-value of 0.00,

indicating that it is the most dominant factor. Higher agitation speed enhances mass transfer between the solid and liquid phases, increasing extraction efficiency. Furthermore, the interaction between solvent type and agitation speed is also significant ($F = 1109.18 > 2.11$; $P = 0.00$), showing that the effect of solvent type depends on the agitation conditions. Therefore, optimizing both solvent selection and agitation speed is crucial for maximizing extraction performance.

3.2 Extraction kinetics

Figures 3 and 4 present the first-order and second-order kinetic models. Kinetic parameters were calculated from the slope and intercept of each linear plot, while the coefficient of determination (R^2) was used to select the most suitable model [11].

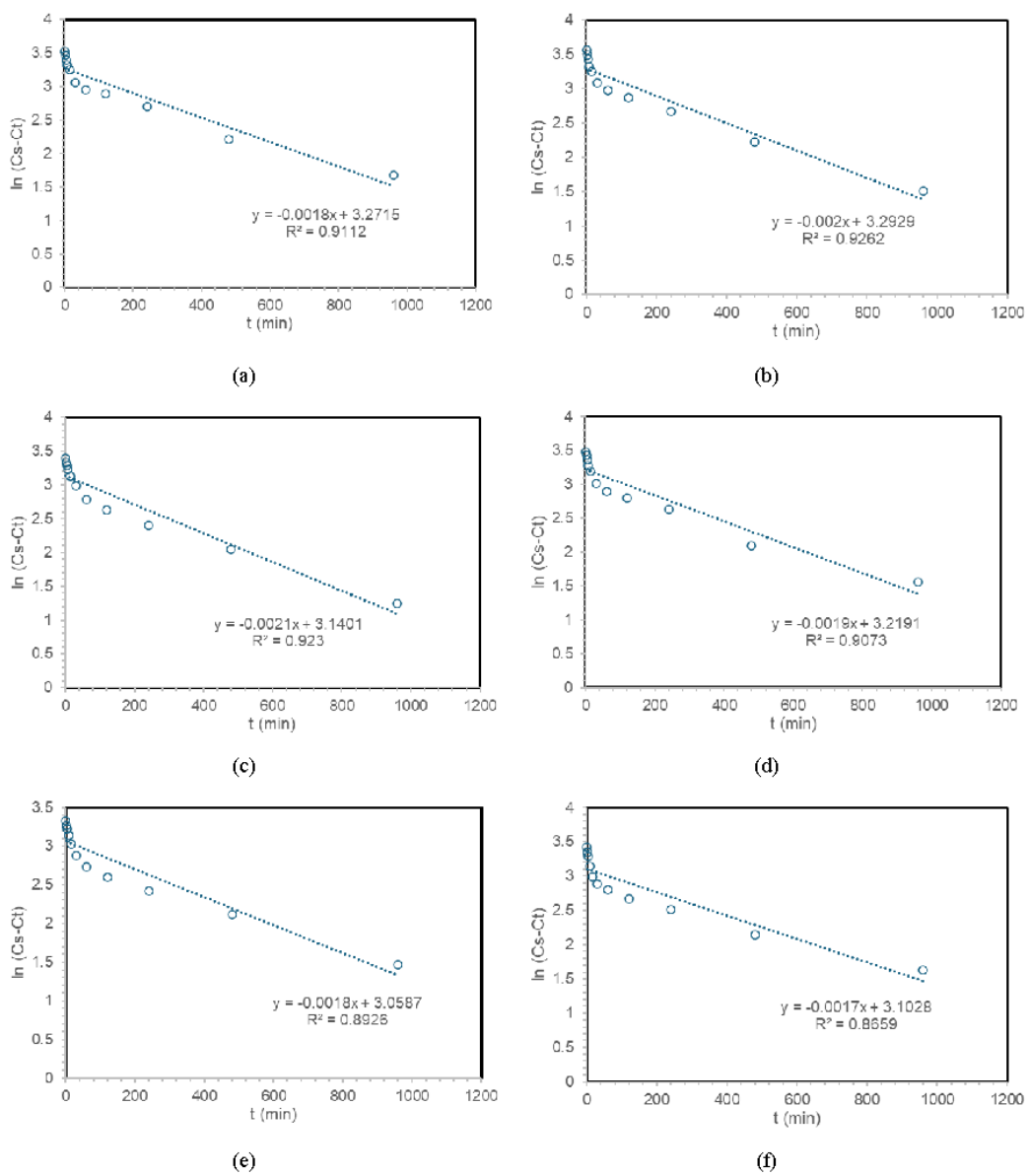


Figure 3. Linear plots of the first-order kinetic model for tin extraction from DMT by-products: (a) water solvent at 300 rpm; (b) water solvent at 400 rpm; (c) 50% methanol solvent at 300 rpm; (d) 50% methanol solvent at 400 rpm; (e) pure methanol solvent at 300 rpm; (f) pure methanol solvent at 400 rpm

The second-order kinetic model produced the highest R^2 values, indicating that it better predicts the extraction behavior. The kinetic parameters (k and C_s) in the second-order model were generally larger than those in the first-order model. First-order R^2 values ranged from 0.86 to 0.92, while second-order values exceeded 0.98. Based on these R^2 values, the second-order model more accurately represents the extraction rate of tin from the DMT by-product.

However, RMSE values in Table 3 show that the second-order model produced larger RMSE values, meaning poorer numerical fit despite a high R^2 . Ideally, smaller RMSE values indicate better model accuracy [12].

Table 3. Kinetic parameters of the first-order and second-order extraction models using the linear method

No	Solvents	rpm	Kinetic models	k	C_s	R^2	RMSE
1	Water	300	First order	0.002	26.330	0.911	8.364
2	Water	300	Second order	0.000	33.560	0.980	14.549
3	Water	400	First order	0.002	26.900	0.926	8.958
4	Water	400	Second order	0.000	35.090	0.984	15.022
5	Methanol 50%	300	First order	0.002	23.120	0.923	7.138
6	Methanol 50%	300	Second order	0.000	29.760	0.988	12.665
7	Methanol 50%	400	First order	0.002	24.990	0.907	8.190
8	Methanol 50%	400	Second order	0.000	32.260	0.983	13.628
9	Methanol	300	First order	0.002	21.320	0.893	7.196
10	Methanol	300	Second order	0.000	27.400	0.981	10.930
11	Methanol	400	First order	0.002	22.250	0.866	8.799
12	Methanol	400	Second order	0.000	29.590	0.980	11.746

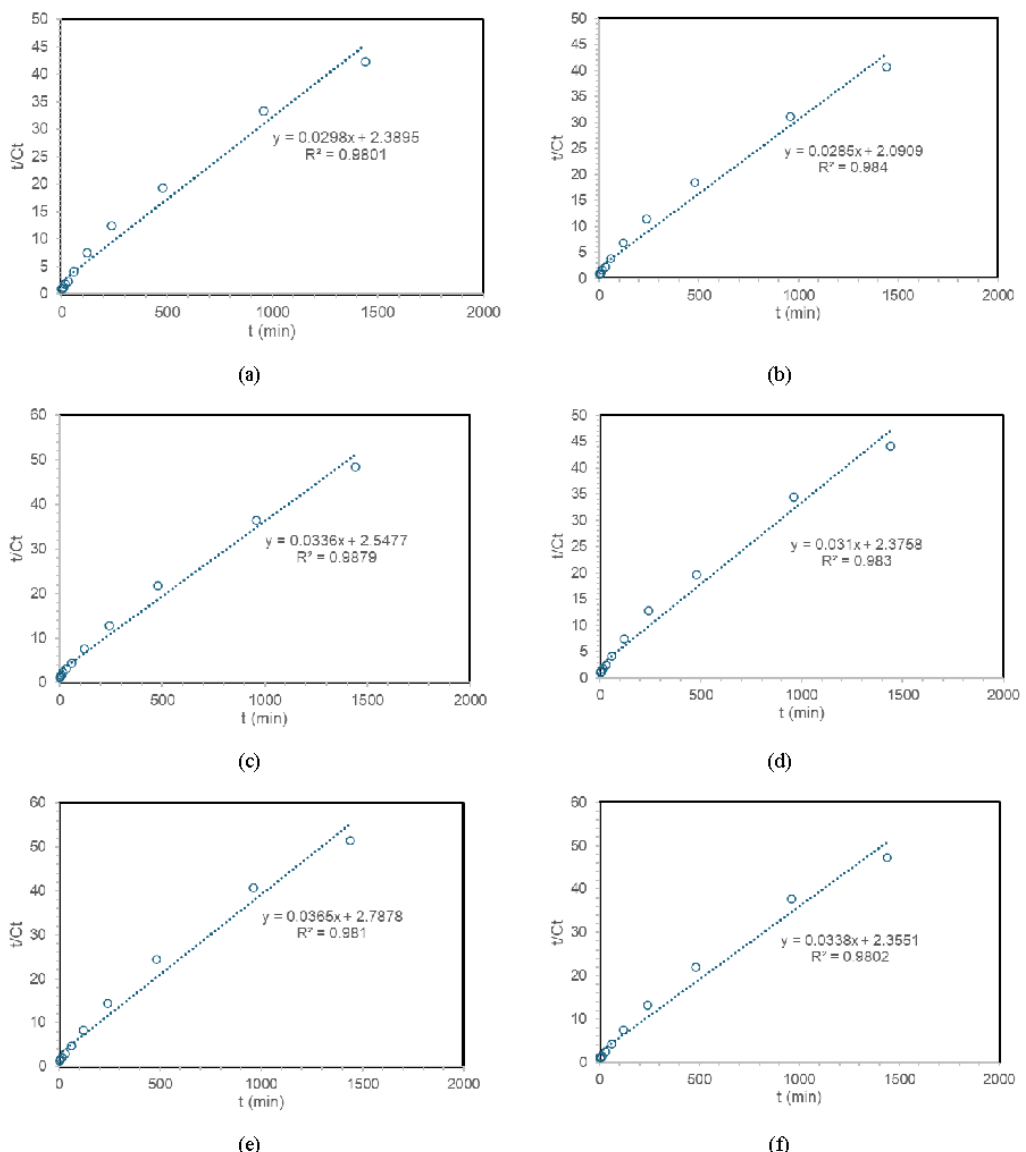


Figure 4. Linear plots of the second-order kinetic model for tin extraction from DMT by-products: (a) water solvent at 300 rpm; (b) water solvent at 400 rpm; (c) 50% methanol solvent at 300 rpm; (d) 50% methanol solvent at 400 rpm; (e) pure methanol solvent at 300 rpm; (f) pure methanol solvent at 400 rpm

This combination of high R^2 but high RMSE suggests that, although the model describes the general trend well, it does not fit the actual data precisely. While linear transformation can distort error distribution, creating misleadingly high R^2 values, nonlinear regression is recommended for more reliable kinetic parameter estimation.

Nonlinear modeling results (Table 4) show that first-order R^2 values remain similar to the linear approach (0.85–0.93), while second-order R^2 values decrease slightly but still remain higher (0.91–0.96). RMSE values are consistently smaller in the second-order model, indicating better model accuracy.

Table 4. Kinetic parameters of the first-order and second-order extraction models using the non-linear method

No	Solvents	rpm	Kinetic models	k	Cs	R ²	RMSE
1	Water	300	First order	0.011	27.340	0.893	3.831
2	Water	300	Second order	0.001	30.090	0.937	2.809
3	Water	400	First order	0.014	28.290	0.890	4.017
4	Water	400	Second order	0.001	31.160	0.938	2.910
5	Methanol 50%	300	First order	0.012	24.660	0.933	2.728
6	Methanol 50%	300	Second order	0.001	27.430	0.969	1.807
7	Methanol 50%	400	First order	0.010	32.650	0.906	5.007
8	Methanol 50%	400	Second order	0.001	28.910	0.941	2.608
9	Methanol	300	First order	0.015	21.910	0.899	2.938
10	Methanol	300	Second order	0.001	24.340	0.946	2.096
11	Methanol	400	First order	0.022	22.870	0.857	3.613
12	Methanol	400	Second order	0.001	25.280	0.918	2.684

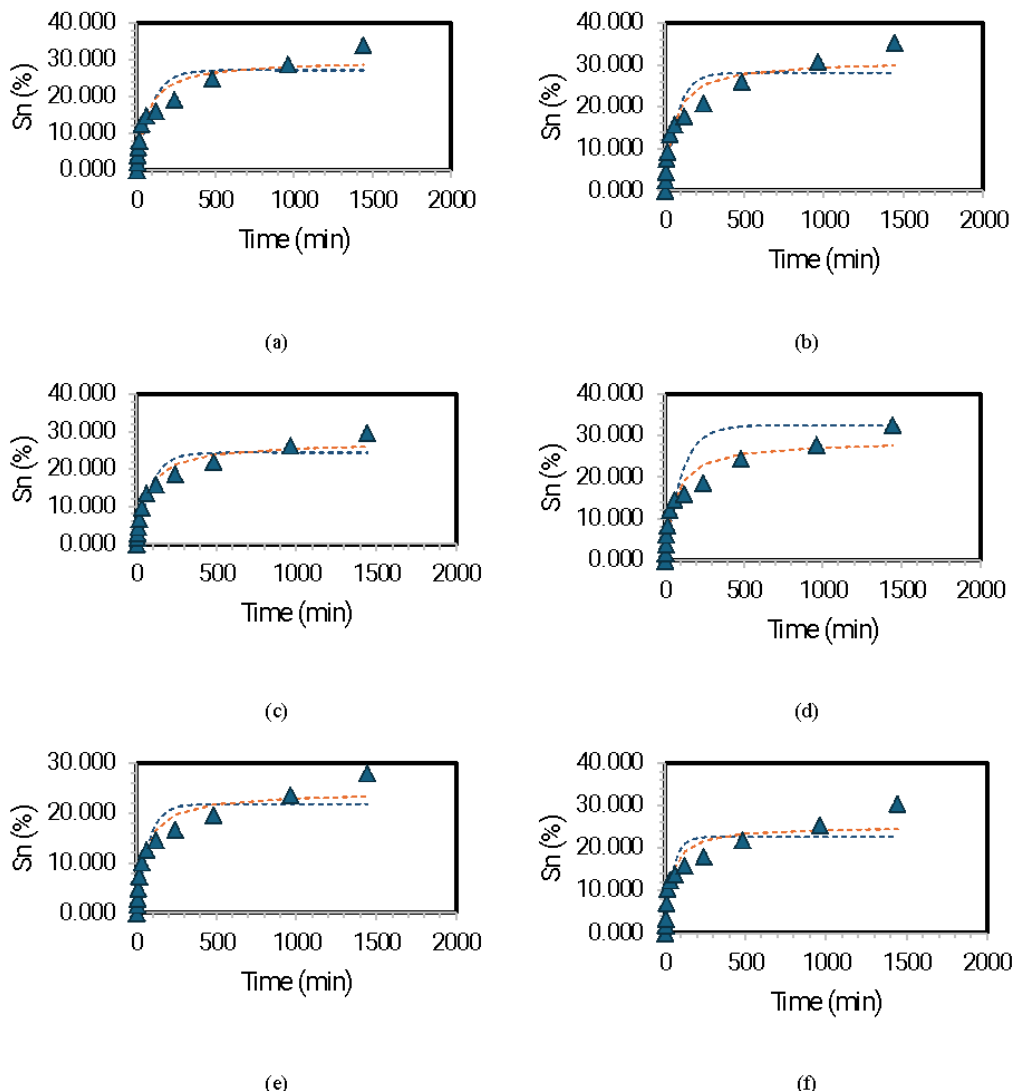


Figure 5. Comparison of experimental data with the non-linear extraction model for tin from DMT by-products: (a) water solvent at 300 rpm; (b) water solvent at 400 rpm; (c) 50% methanol solvent at 300 rpm; (d) 50% methanol solvent at 400 rpm; (e) pure methanol solvent at 300 rpm; (f) pure methanol solvent at 400 rpm (blue dashed line: first-order model, red dashed line: second-order model)

Nonlinear fitting also shows improved correspondence between the model and experimental data (Fig. 5), with reduced deviation compared to the linear approach. Nonlinear regression directly fits the original equation without mathematical transformation, resulting in more accurate and realistic kinetic parameter estimation [7], [12].

The extraction profile previously described, rapid extraction followed by a slower phase (Fig. 2), supports the interpretation that the process follows second-order kinetics. According to [10], second-order solid-liquid extraction kinetics indicate that the rate-limiting mechanism involves surface reactions and film diffusion rather than simple dissolution. This model is commonly

associated with chemisorption-type interactions or strong interactions between solutes and solid surfaces. Second-order kinetics typically describe slower extraction processes and are consistent with long extraction durations [13]. This suggests the need for regime-based modeling to accurately represent the extraction behavior.

The extraction kinetics were further analyzed by separating the process into two regimes: rapid extraction ($t = 0-120$ min) and slow extraction ($t = 240-1440$ min). Figures 6 and 7 show the first- and second-order models under the two-regime approach. The nonlinear regression fitting significantly improved model accuracy for both kinetic models.

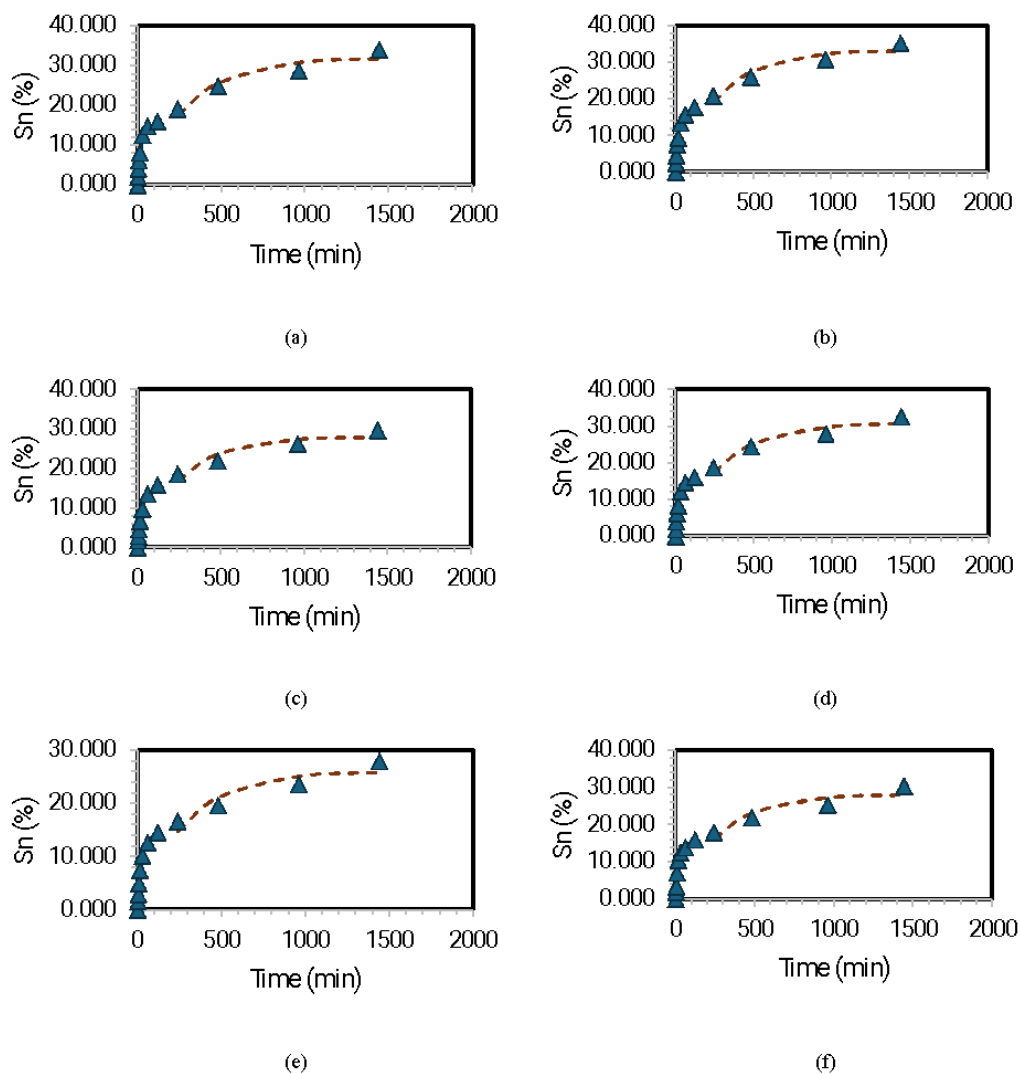


Figure 6. Comparison of experimental data with the first-order extraction model for tin from DMT by-products: (a) water solvent at 300 rpm; (b) water solvent at 400 rpm; (c) 50% methanol solvent at 300 rpm; (d) 50% methanol solvent at 400 rpm; (e) pure methanol solvent at 300 rpm; (f) pure methanol solvent at 400 rpm (blue dashed line: first-order model, red dashed line: second-order model)

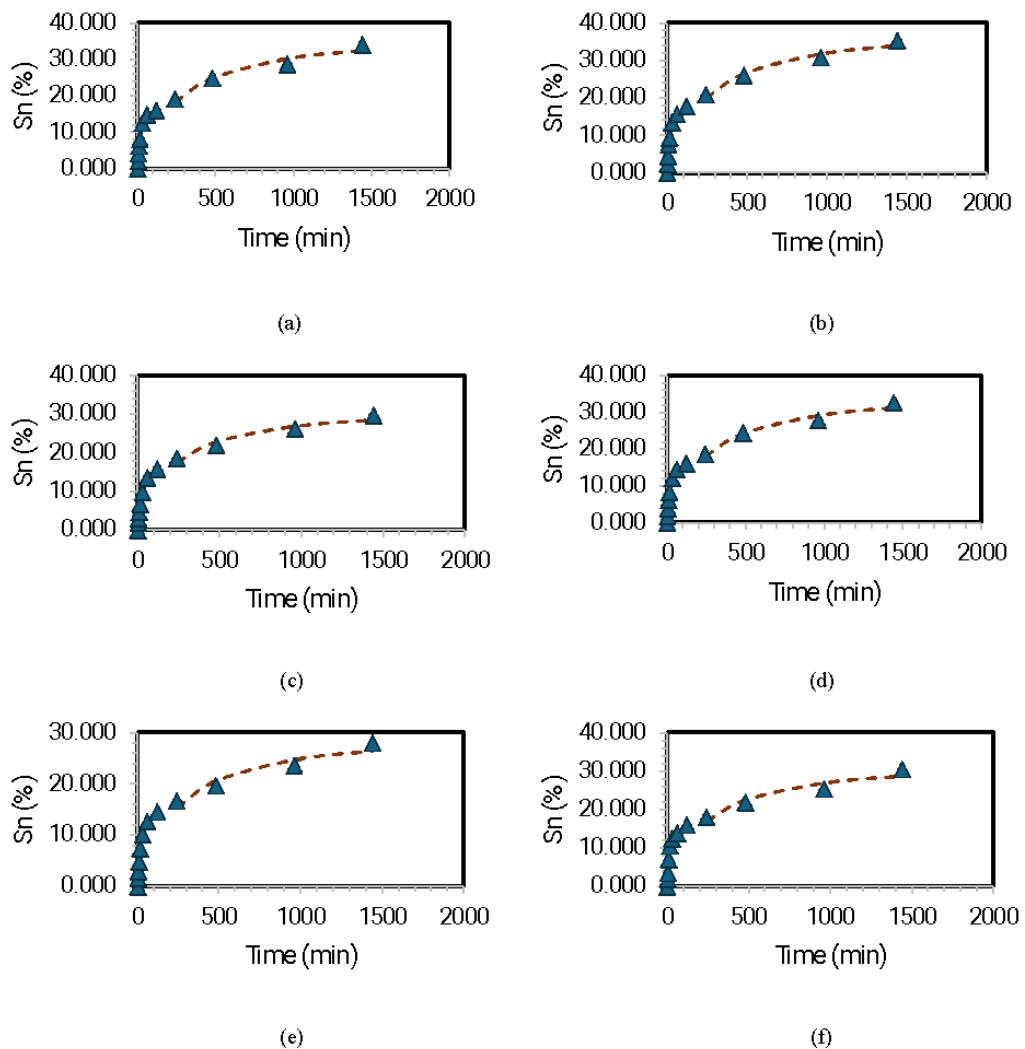


Figure 7. Comparison of experimental data with the second-order extraction model for tin from DMT by-products: (a) water solvent at 300 rpm; (b) water solvent at 400 rpm; (c) 50% methanol solvent at 300 rpm; (d) 50% methanol solvent at 400 rpm; (e) pure methanol solvent at 300 rpm; (f) pure methanol solvent at 400 rpm (blue dashed line: first-order model, red dashed line: second-order model)

The extraction rate constant (k) increased approximately fivefold in the rapid-extraction regime compared to the one-regime model (Table 5). For both orders, the value of k in the fast-extraction regime was consistently higher than in the slow-extraction regime, confirming the transition from fast surface release to diffusion-controlled extraction. According to [8], higher k -values reflect faster diffusion and evaporation processes, while lower values correspond to diffusion-limited stages.

In the two-regime model, the first-order R^2 increased substantially, reaching >0.99 in the rapid-extraction regime, approaching the R^2 of the second-order model. In the slow regime, R^2 values for both models decreased, but the second-order model still provided a better fit (Table 6). RMSE values consistently show that the second-order model yields lower RMSE in both regimes, reinforcing that second-order kinetics best represent the extraction behavior.

Table 5. Kinetic parameters of the first-order and second-order extraction models in the rapid-extraction stage (short-time regime)

No	Solvents	rpm	Kinetic models	k	C_s	R^2	RMSE
1	Water	300	First order	0.0567	15.632	0.992	0.538
2	Water	300	Second order	0.0034	18.435	0.995	0.394
3	Water	400	First order	0.0623	16.769	0.990	0.752
4	Water	400	Second order	0.0036	19.636	0.997	0.335
5	Methanol 50%	300	First order	0.0373	15.608	0.993	0.548
6	Methanol 50%	300	Second order	0.0020	19.276	0.997	0.307
7	Methanol 50%	400	First order	0.0556	15.541	0.994	0.507
8	Methanol 50%	400	Second order	0.0033	18.412	0.998	0.243
9	Methanol	300	First order	0.0487	13.973	0.997	0.446
10	Methanol	300	Second order	0.0031	16.826	1.000	0.064
11	Methanol	400	First order	0.0745	14.877	0.992	0.614
12	Methanol	400	Second order	0.0047	17.426	0.992	0.526

The second-order extraction behavior is also linked to possible partial hydrolysis of organotin compounds during extraction. [13] suggests that

second-order kinetics may involve hydrolysis of organic species during solid–liquid extraction. According to [14], dissolved organotin species exhibit Lewis acidity with different hardness levels ($\text{RSn}^{3+} > \text{R}_2\text{Sn}^{2+} > \text{R}_3\text{Sn}^+$), and all undergo hydrolysis to varying extents in aqueous solutions (Table 7).

Table 6. Kinetic parameters of the first-order and second-order extraction models in the slow-extraction stage (long-time regime)

No	Solvents	rpm	Kinetic models	k	C _s	R ²	RMSE
1	Water	300	First order	0.0034	32.228	0.905	1.726
2	Water	300	Second order	0.0001	38.546	0.958	1.118
3	Water	400	First order	0.0036	33.627	0.911	1.676
4	Water	400	Second order	0.0001	39.747	0.969	0.954
5	Methanol 50%	300	First order	0.0039	28.146	0.869	1.587
6	Methanol 50%	300	Second order	0.0002	32.751	0.951	0.941
7	Methanol 50%	400	First order	0.0035	30.922	0.924	1.462
8	Methanol 50%	400	Second order	0.0001	36.757	0.964	0.969
9	Methanol	300	First order	0.0035	26.192	0.844	1.761
10	Methanol	300	Second order	0.0001	30.988	0.923	1.190
11	Methanol	400	First order	0.0036	28.352	0.842	1.884
12	Methanol	400	Second order	0.0001	33.470	0.921	1.289

However, the hydrolysis behavior reported by [14] occurs at moderate pH values (pH 2–4.5). This contradicts the results of this study, where the extract solutions show much lower pH values (pH 0.81–1.65). At such strongly acidic conditions, hydrolysis is suppressed because water cannot act as a nucleophile due to the high proton concentration.

Any partially hydrolyzed species (e.g., $\text{RSnCl}_2(\text{OH})$, $\text{R}_2\text{SnCl}(\text{OH})$) would immediately reprotonate, reverting to their original halide forms. Consequently, the dominant species under these conditions are organotin halides such as DMT (R_2SnCl_2) and MMT (RSnCl_3), with minimal hydrolysis. Therefore, the extraction mechanism remains governed by surface reaction and film diffusion, consistent with second-order kinetics.

Table 7. Hydrolytic species formed under low organotin concentration conditions

Kation organotin	Spesies hidrolitik yang terbentuk
RSn^{3+}	$[\text{RSn}(\text{OH})]^{2-}$, $[\text{RSn}(\text{OH})_2]^+$, $[\text{RSn}(\text{OH})_3]^0$, $[\text{RSn}(\text{OH})_4]^-$, $[(\text{RSn})_2(\text{OH})_3]^+$
R_2Sn^{2+}	$[(\text{R}_2\text{Sn})(\text{OH})]^+$, $[\text{R}_2\text{Sn}(\text{OH})_2]^0$, $[\text{R}_2\text{Sn}(\text{OH})_3]^-$, $[(\text{R}_2\text{Sn})_2(\text{OH})_2]^{2-}$, $[(\text{R}_2\text{Sn})_2(\text{OH})_3]^+$
R_3Sn^+	$[\text{R}_3\text{Sn}(\text{OH})]^0$, $[\text{R}_3\text{Sn}(\text{OH})_2]^-$

The transition between the rapid and slow extraction phases observed mathematically can be elucidated through the physical mechanism illustrated in Fig. 8. In the initial stage (fast regime), the solutes (indicated as red dots) are concentrated on the particle surface or near the

pore openings, making them highly accessible to the solvent. This is represented by the bold black arrows in the schematic, indicating the dominance of the surface reaction mechanism with high rate constants (k) during the first 120 minutes.

As the process continues, it enters the final stage (slow regime), where the remaining solutes are located deep within the solid matrix or trapped within internal structures. This phenomenon is depicted by the thin, wavy arrows, symbolizing resistance from film diffusion and intraparticle diffusion.

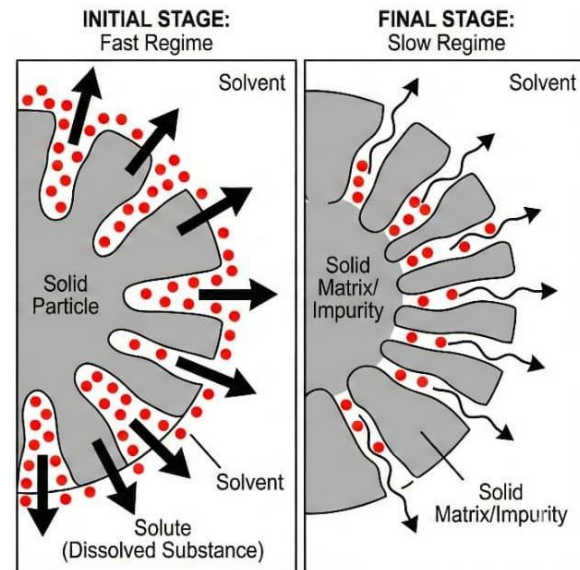


Figure 8. Schematic representation of the two-regime extraction mechanism for DMT by-product

The superior fit of the second-order kinetic model (lower RMSE) at this stage reinforces the evidence that the extraction rate is limited by physical mass transfer barriers of the solute from the matrix to the solvent, rather than simple dissolution. Furthermore, the stability of DMT and MMT species under strongly acidic conditions (pH 0.81–1.65) ensures that the illustrated diffusion pathways remain focused on the mass transfer of halide species without interference from hydrolysis products.

4. CONCLUSION

This study demonstrates that solvent polarity and agitation intensity play a critical role in governing tin extraction from DMT (dimethyltin dichloride) by-products. Water preferentially enhances inorganic tin dissolution, whereas methanol favors the extraction of organotin species. The extraction kinetics consistently follow a pseudo-second-order model, with nonlinear regression providing more reliable kinetic parameters than linear fitting. The distinction between short-time surface-controlled

and long-time diffusion-controlled regimes further strengthens the mechanistic interpretation of the extraction process.

Theoretically, this work refines the kinetic modeling of organotin residues by validating a regime-based analysis over traditional single-regime interpretations. Overall, optimizing these conditions significantly improves tin recovery, highlighting the potential of DMT by-products as viable secondary resources. Future research should explore temperature-dependent kinetics and advanced speciation analysis to further optimize industrial-scale recovery technologies.

ACKNOWLEDGEMENT

We gratefully acknowledge PT Timah Industri for research funding support through “Kegiatan kerja sama penelitian PT Timah Industri – Untirta” (No. 006/TI/SPK-2000/2024-S0 and 840/UN43/HK.06.00/2024.

REFERENCES

- [1] L. O. Arham, “Studi perolehan kembali timah dari produk samping kerak reaktor pembuatan organotin asal PT Timah Industri dengan metode pelindian menggunakan asam sulfat dan electrowinning,” *Tesis, Institut Teknologi Bandung*, Bandung, Indonesia, 2018.
- [2] Fisher Scientific, “Dimethyltin dichloride”, fishersci.fi, 2025. [Online]. Available: <https://www.fishersci.fi/shop/products/dimethyltin-dichloride-thermo-scientific/11364829>. [Accessed: Dec. 10, 2025].
- [3] Fisher Scientific, “Methyltin trichloride, 97%, Thermo Scientific Chemicals”, fishersci.com, 2025. [Online]. Available: <https://www.fishersci.com/shop/products/methyltin-trichloride-97-thermo-scientific/AA7115603>. [Accessed: Dec. 10, 2025].
- [4] Fisher Scientific, “Tin (II) oxide, 99%”, fischersci.be, 2025. [Online]. Available: <https://www.fishersci.be/shop/products/tin-ii-oxide-99-thermo-scientific/11483498>. [Accessed: Dec. 10, 2025].
- [5] Fisher Scientific, “Tin (IV) oxide, 99.9% (metals basis)”, fischersci.pt, 2025. [Online]. Available: <https://www.fishersci.pt/shop/products/tin-iv-oxide-99-9-metals-basis-thermo-scientific/p-4904556>. [Accessed: Dec. 10, 2025].
- [6] A. J. Tušek, M. Benković, A. B. Cvitanović, D. Valinger, T. Jurina, and J. G. Kljusurić, “Kinetics and thermodynamics of the solid-liquid extraction process of total polyphenols, antioxidants and extraction yield from asteraceae plants,” *Ind. Crops Prod.*, vol. 91, pp. 205-214, 2016. DOI: 10.1016/j.indcrop.2016.07.015.
- [7] A. M. Kisiela-Czajka and B. Dziejarski, “Linear and non-linear regression analysis for the Adsorption Kinetics of SO₂ in a fixed carbon bed reactor-A case study,” *Energies (Basel)*, vol. 15, no. 2, 2022. DOI: 10.3390/en15020633.
- [8] Satriana, A. Maulida, R. Qardhawi, Y. M. Lubis, R. Moulana, W. A. W. Mustapha, and N. Arpi, “Study of solid–liquid extraction kinetics of oil from dried avocado (*Persea Americana*) flesh using hexane as a solvent,” *International Journal of Technology*, vol. 14, no. 5, pp. 982-992, 2023. DOI: 10.14716/ijtech.v14i5.6370.
- [9] P. Hobbi, O. V. Okoro, C. Delporte, H. Alimoradi, D. Podstawczyk, L. Nie, K. V. Bernaerts, and A. Shavandi, “Kinetic modelling of the solid–liquid extraction process of polyphenolic compounds from apple pomace: influence of solvent composition and temperature,” *Bioresour Bioprocess*, vol. 8, no. 1, 2021. DOI: 10.1186/s40643-021-00465-4.
- [10] Y.S. Ho and G. McKay, “Pseudo second order model for sorption processes,” *Process Biochemistry*, vol. 34, pp. 451-465, 1999. DOI: 10.1016/S0032-9592(98)00112-5.
- [11] A. F. Arimalala, R. P. Herve, and R. Rafihavavana, “Modeling and kinetics study of avocado oil extraction from Madagascar using different mathematical models,” *S. Afr. J. Chem. Eng.*, vol. 41, pp. 93-97, 2022. DOI: 10.1016/j.sajce.2022.05.006.
- [12] S. Ahmadi, C. A. Igwegbe, S. Rahdar, and Z. Asadi, “The survey of application of the linear and nonlinear kinetic models for the adsorption of nickel(II) by modified multi-walled carbon nanotubes,” *Appl. Water Sci.*, vol. 9, no. 4, Jun. 2019. DOI: 10.1007/s13201-019-0978-9.
- [13] M. E. Yulianto, R. D. Nyamiati, and M. Mustikaningrum, “Kinetics modelling of the solid-liquid extraction process of linamarin compounds from cassava leaves assisted by UV-Photobioextractor,” in *Materials Today: Proceedings*, Elsevier Ltd, pp. 230-233, 2023. DOI: 10.1016/j.matpr.2023.03.099.
- [14] C. Brett, R. Cigala, and A. Giacalone, “Hydrolysis of organotin compounds at

high concentration,” in *Proc. XVIII Italian-Spanish Congress on Thermodynamics of Metal Complexes (SIMEC)*, 2008.

